

# The filtering of layover areas in high-resolution IFSAR for the building extraction.

D. Petit (ab)<sup>\*1</sup>, F. Adragna (a)<sup>\*2</sup>, J.D. Durou (b)<sup>\*3</sup>  
(a: Centre National d'Etudes Spatiales, Toulouse, France)  
(b: Institut de Recherche en Informatique, Toulouse, France)

## ABSTRACT

The capabilities of Interferometric SAR (IFSAR) to provide Digital Elevation Model is well known and have been highlighted with the recent Shuttle Radar Topographic Mission. Nevertheless, layovers, shadows, multiple bounces and surfaces discontinuity strongly reduce the accuracy of the extracted shapes in urban areas with high-resolution systems.

Due to the number and the complexity of uncontrolled interactions at work, we choose to use simulations to study the layover produced by buildings. An interferogram simulator developed at CNES, IRIT and CS, which is called 2SIR, can achieve those. This tool has been designed in order to simulate realistic interferograms (and its pair of radar images) in such complex situations as urban areas.

C. Prati et al. have shown that a slope induces a spectral shift of the ground response. Although it generates a loss of coherence, it can be used to partially separate layover and non layover areas as they done with ERS images. In high-resolution, the spectral shift is insufficient to apply such a filtering. However, this technique can be achieved in urban area with certain restrictions to extract the shape of buildings.

**Keywords:** Layover, IFSAR, urban, 3D, filtering, interferometry, slope, spectral shift.

## 1. INTRODUCTION

Nowadays, the Interferometric SAR (IFSAR) are commonly used to provide Digital Elevation Model quickly and accurately, especially where a permanent band cloud disables other techniques. The new or future high-resolution systems (few meters and less) allow theoretically extracting the shape of buildings in urban areas. Nevertheless, layovers, shadows, multiple bounces and surfaces discontinuity strongly reduce the accuracy of this technique. In order to improve the performances, those phenomena must be separated or filtered, to be processed suitably.

Basically, in urban areas, layover is one of the most restricting problem as it has been underlined by P. Gamba et al.<sup>1</sup> or D.L. Bickel et al.<sup>2</sup>. It is obvious indeed that each building we want to extract, generates a layover case. Classical algorithms are not able to unwrap the phase correctly in those areas. Three signals are not only superposed, but one of them is reversed. Therefore, a specific treatment is required. This is what we have studied in the particular case of building layover.

The second part is a reminder of the theory of the spectral shift. The third part explains how to use this theory to filter a particular slope. Limitations of the unwrapping in the building layovers are exposed in the fourth part. This research is based on simulations done by 2SIR (part five), and some results are discussed in part six. We conclude on this promising method in the final part.

## 2. THEORY OF THE SPECTRAL SHIFT

### 1 The spectral shift

C. Prati et al.<sup>3</sup> have shown that a slope induces a spectral shift of the ground response. Although it generates a loss of coherence, F. Gatelli et al.<sup>4</sup> show that it can be used to partially separate layover and non layover areas (as they done with ERS images) or to improve the slant range resolution.

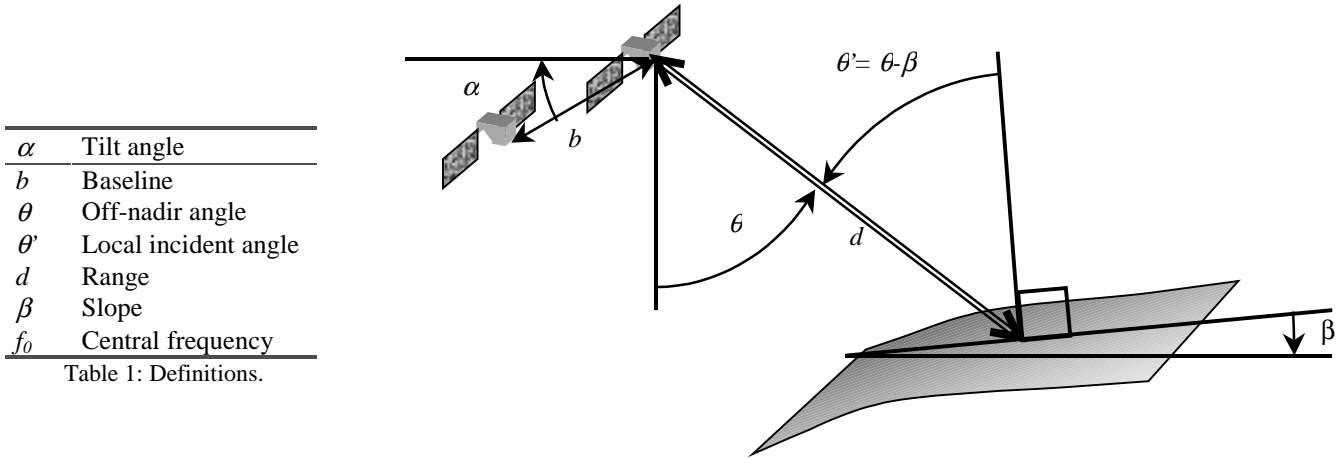
---

<sup>\*1</sup> email: [David.Petit@irit.fr](mailto:David.Petit@irit.fr), WEB site: <http://www.irit.fr/~David.Petit>.

<sup>\*2</sup> email: [Frederic.Adragna@cnes.fr](mailto:Frederic.Adragna@cnes.fr).

<sup>\*3</sup> email: [Jean-Denis.Durou@irit.fr](mailto:Jean-Denis.Durou@irit.fr).

Figure 1 shows the geometry of an IFSAR acquisition. The spectral shift of the ground response can be estimated by the equation (1).



$\alpha$	Tilt angle
$b$	Baseline
$\theta$	Off-nadir angle
$\theta'$	Local incident angle
$d$	Range
$\beta$	Slope
$f_0$	Central frequency

Table 1: Definitions.

Fig. 1: IFSAR geometry

$$\Delta f = f_0 \frac{b \cos(\theta - \alpha)}{kd \tan(\theta - \beta)} \quad (1)$$

The value of the parameter  $k$  is 2 in the bistatic case, and 1 in the monostatic case. This formula can be demonstrated by several ways, one of them is to consider the classical decomposition of the radar phase:

$$\phi_{total} = \phi_{distance} + \phi_{instrument} + \phi_{atmospheric} + \phi_{construction} + \phi_{backscattering} + \phi_{noise} \quad (2)$$

The DEM reconstruction using IFSAR system expects that all components are constant, but the phase is linked to the distance. It allows computing the distance difference associated to the phase difference. However, the construction phase depends how echoes returned within a pixel are added. Let us consider two targets placed within a pixel. The construction phase is linked to the phase difference between the two returned echoes. If we call  $l$  the range difference, the phase difference  $\Delta\phi$  in the case of figure 2a is given by (3) whereas it is given by (4) for a small variation  $\delta\theta'$  of incident angle, as described in figure 2b.

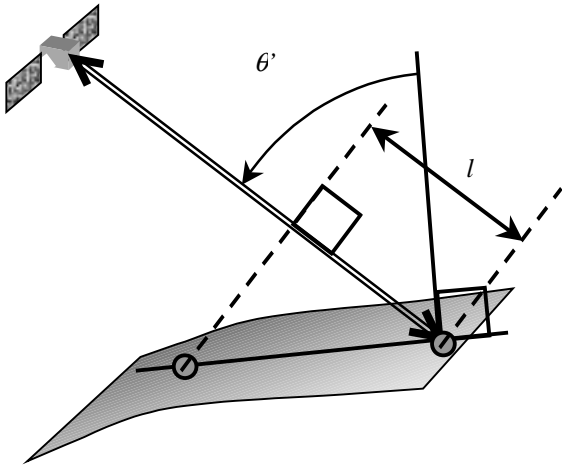


Fig. 2a: Dephasing between two targets

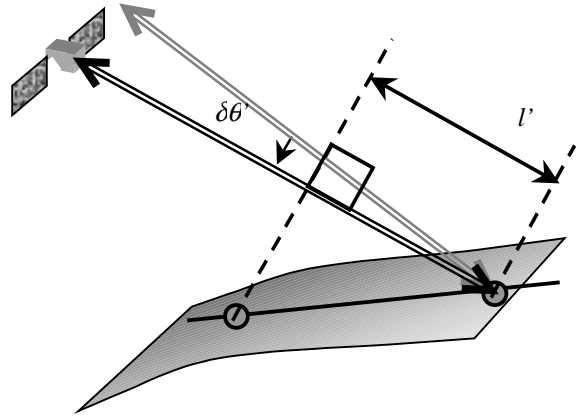


Fig 2b: Dephasing with a different incident angle.

$$\Delta\phi = 2\pi \frac{f_0}{c} 2l \quad (3)$$

$$\Delta\phi' = 2\pi \frac{f_0}{c} 2l' \quad (4)$$

In the monostatic case, the construction phase is constant if only (5) is true, that is impossible unless we assume that the frequency is not the same in the second acquisition.

$$\Delta\phi = \Delta\phi' \quad (5)$$

We know (6) and if we suppose (7), we get (9). These formulae can be easily extended to the bistatic case so as to obtain (1).

$$l' \sin(\theta' + \delta\theta') = l \sin(\theta') \quad (6)$$

$$\theta' \neq 0 \quad \text{and} \quad \delta\theta' \ll 1 \quad (7)$$

$$\Delta\phi' = \frac{4\pi f_0' l}{c [1 + \delta\theta' / \tan(\theta')]} = \Delta\phi = \frac{4\pi f_0 l}{c} \quad (8)$$

$$\Rightarrow f_0' = f_0 [1 + \delta\theta' / \tan(\theta')] \Rightarrow \Delta f = f_0 \frac{\delta\theta'}{\tan(\theta')} \quad (9)$$

In order to maintain the construction phase constant, the central frequency could be shifted. However this correction is not well opportune since this shift depends on the slope  $\beta$ . Moreover, the difference of distance phase would be null too, if the spectral shift is compensated by a shift of the central frequency. That would lead to make interferometric applications unfeasible! Also the construction phase depend on geometrical condition of acquisitions.

## 2 Limitation of the interferometry

In fact, the larger the baseline, the worst the spectral responses match. The unmatched spectral responses are not correlated. It induces that a phase noise is added, which decreases the coherence of the final interferogram. The limit when the spectral responses are totally separated, fixes a maximum baseline as shown by C. Prati et al.<sup>3,4</sup>. F. Adragna reminds in the bulletin of the SFPT<sup>5</sup> that this is the first limitation of interferometric techniques with spatial systems. If  $B$  is the bandwidth and  $R_d$  the resulting slant range resolution, we can deduce a critical orthogonal baseline  $b_\perp$  ( $b_\perp = b \cos(\theta - \beta)$ ) from (1):

$$|\Delta f| < B \Rightarrow \left| \frac{f_0 b_\perp}{kd \tan(\theta')} \right| < \frac{c}{2R_d} \Rightarrow b_\perp < \frac{kd\lambda |\tan(\theta')|}{2R_d} \quad (10)$$

$$b_\perp < \frac{kd\lambda |\tan(\theta - \beta)|}{2R_d} \quad (11)$$

Also, the interferometric quality decreases as the orthogonal baseline increases. The interferometric quality can be estimated by the function of coherence<sup>9</sup> (12), where  $\Phi$  is a fringe model. The function  $\Phi$  can be a simple plane of phase drawn from the computation of the mean gradient (13).  $\Phi$  is a scalar product between the mean gradient of fringe and a vector of index  $(i, j)$ . Components of this vector are the relative indexes of a pixel in the window within the coherence is assessed.

$$\tilde{\gamma} = \frac{\langle x_1 \cdot x_2^* \cdot \exp(-i\Phi) \rangle}{\sqrt{\langle x_1 \cdot x_1^* \rangle \langle x_2 \cdot x_2^* \rangle}} \quad (12)$$

$$\Phi = \left\langle \nabla \text{Phase} \left( \frac{x_1 \cdot x_2^*}{\sqrt{x_1 \cdot x_1^* \cdot x_2 \cdot x_2^*}} \right) \right\rangle \cdot (i \quad j) \quad (13)$$

So as to improve the coherence, it is interesting to eliminate spectral bands that do not match. This is what DIAPASON<sup>6</sup> do. DIAPASON is an interferometric chain, developed at CNES. It is designed to take into account the slope in the computation of interferograms (and also coherence images), by an adaptive spectral filtering of source radar image.

### 3. THE SLOPE SELECTION

#### 1 Slope interferogram

C. Prati, F Gatelli et al.<sup>3,4</sup> show that the spectral filtering can be used to partially separate layover and non layover areas, and they did it with ERS images. It seems possible to use this method to filter radar images with the aim to get the interferogram related to a particular slope, which we will call slope interferogram

Let us take two images holding a signal related to a specific slope. There is a spectral shift  $\Delta f$  between the two spectral responses of the surface. We select on each image a part of the signal with a bandwidth of  $\Delta f$ , and a spectral shift of  $\Delta f$  between them. If we compute the interferogram, as spectral responses match exactly, the coherence has consequently to be excellent. If an other signal corresponding to an other slope was mixed, an incoherent interferogram will be superposed. The consequent interferogram has therefore a debased resolution, and the coherence is all the more low that the source images was composed of different slope contributions.

However, we can compute other interferograms by shifting the two-selected band. Each sub-interferogram contains the coherent interferogram related to the selected slope and an incoherent interferogram, which can be comparable at a phase noise. Thus, we can add each sub-interferogram to lower this undesirable contribution as described in figure 3.

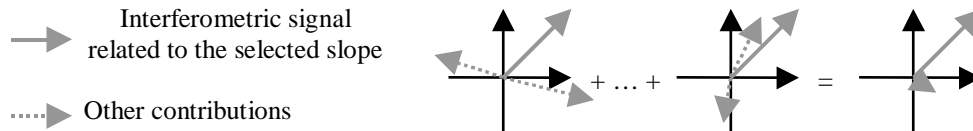


Fig 3: Summation of each sub-interferogram in Fresnel representation.

Therefore, this process can be exploited to select the interferogram related to a specific slope signal. In case of layover, if the two slopes are known, we can separate two slope interferograms.

#### 2 Separating two slope interferograms

In order to simplify the problem, we choose the incident angle  $\theta$  equal to 45 degrees. We suppose that we have a horizontal and vertical plane. We can simplify (1) to obtain (14).

$$\Delta f = \pm f_0 \frac{b_{\perp}}{kd} \quad (14)$$

As explained before and shown in figure 4, we can compute sub-interferograms for each slope. The slave image produces two filtered images, which we make interfere with the filtered master image. Each sub-interferogram is added to generate two slope interferograms. We also subtract the phase plane that each slope engenders, with the aim to easily unwrap the phase, later.

The slope of the phase plane can be deduced from the well-known geometrical definition of interferometric phase (15). If we consider a little displacement in range of  $\delta i$  pixel,  $\Phi$  varies with  $\theta$  like in (16). For a slope  $\beta$ , we know variations of  $\theta$  (17). Hence, the phase gradient for a slope  $\beta$  is described by (18).

$$\Phi = \Delta\phi = 4\pi b \sin(\theta - \alpha) / (k\lambda) \quad (15)$$

$$\delta\Phi / \delta i = (4\pi b \cos(\theta - \alpha)) / (k\lambda) \delta\theta / \delta i \quad (16)$$

$$\delta\theta / \delta i = S_d / (d \tan(\theta - \beta)) \quad (17)$$

$$\delta\Phi / \delta i = (4\pi b S_d \cos(\theta - \alpha)) / (k\lambda d \tan(\theta - \beta)) \quad (18)$$

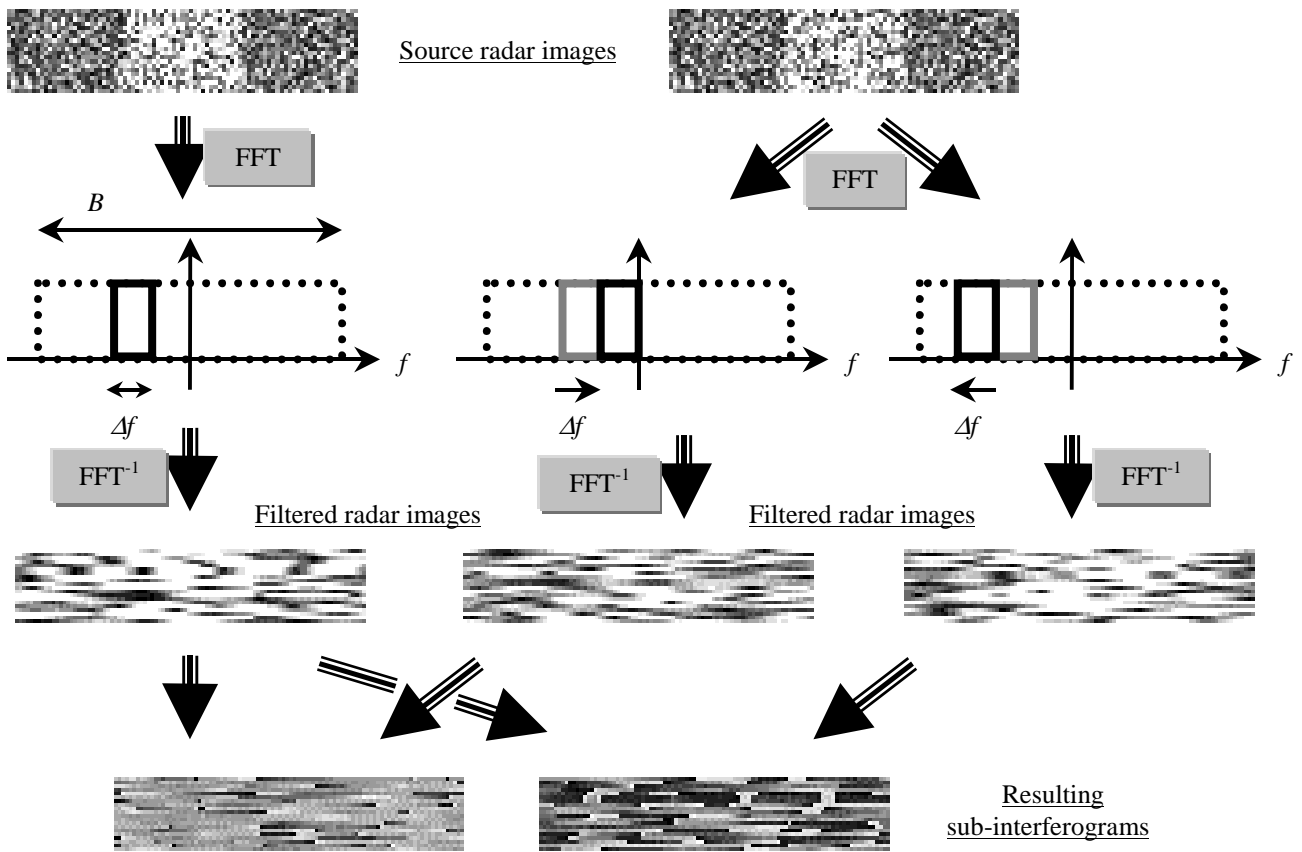


Fig 4: production of sub-interferograms.

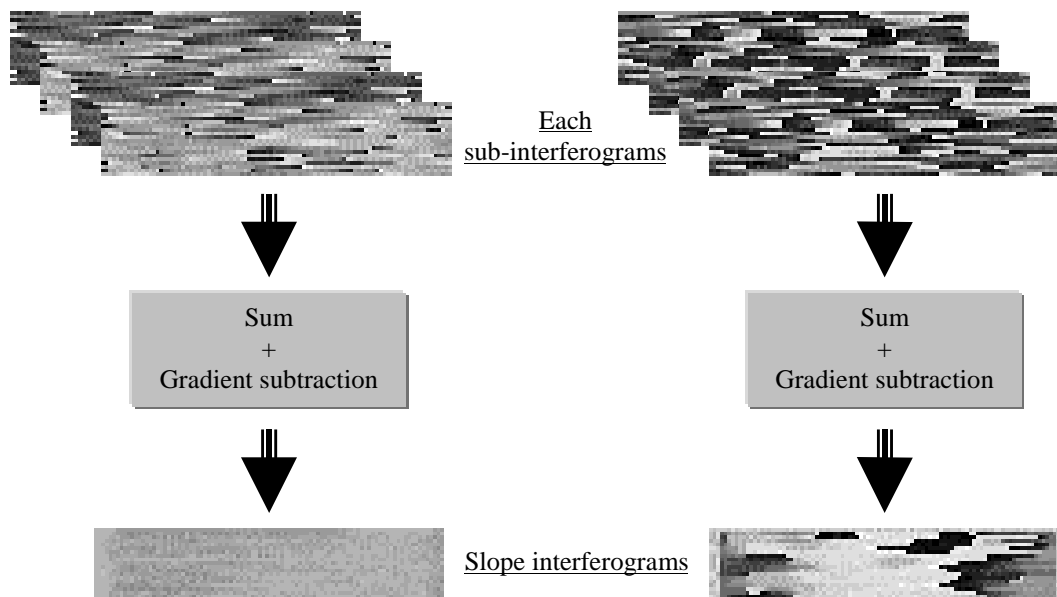


Fig 5: Production of slope interferograms.

## 4. UNWRAPPING IN THE BUILDING LAYOVERS

### 1 Limits

We saw how to separate slope interferograms for horizontal and vertical planes, so in case of building layover. Nevertheless, this method requires a minimal spectral shift in relation to the sampling Frequency  $F_s$  (and also the slant range sampling  $S_d$ ). If  $N$  is the size in pixel of the layover region,  $\Delta f$  must verify (19). A lesser shift would be insufficient to allow the filtering. Besides a value higher than  $F_s/2$  would decrease the efficiency of the process.

$$\frac{F_s}{N} < \Delta f < \frac{F_s}{2} \quad (19)$$

We can reformulate this limitation by using the altitude of ambiguity  $E_a$ . This is a convenient parameter introduced by D. Massonnet<sup>7</sup>, which provide a quick assessment of the influence of a given geometry with respect to radar interferometry. The altitude of ambiguity represents a round trip range variation equal to the radar wavelength. Its expression (19), gives a new definition of the spectral shift (20). Hence, if  $W$  is the width in range of layover area, we obtain the formulae (21) and (22).

$$E_a = \frac{k\lambda d \sin(\theta^*)}{2b_\perp} \quad (19)$$

$$\Delta f = \frac{c \cos(\theta^*)}{2E_a} \quad (20)$$

$$\frac{1}{NS_d} < \frac{\cos(\theta^*)}{E_a} < \frac{1}{2S_d} \Rightarrow 2S_d < \frac{E_a}{\cos(\theta^*)} < NS_d \quad (21)$$

$$2S_d < \frac{E_a}{\cos(\theta^*)} < W \quad (22)$$

We can simplify this expression if we assume that incident angle is equal to 45 degrees, and the layover is made by a building of height  $H$ . Therefore, the process can be suitably applied if the altitude of ambiguity  $E_a$  verify the inequality (23).

$$\sqrt{2}S_d < E_a < \frac{H}{2} \quad (23)$$

### 2 A Method for unwrapping in the building layover

We know that coherence is lesser in layover areas<sup>8</sup>, and classical techniques are unable to unwrap the phase suitably, in those regions. In slope interferograms, the coherence related to a slope is improved. In figures 6, we have simulations of coherence after a slope filtering. Each image can be divided in three parts: the central part is a presumed layover area, the two other parts are areas of horizontal planes.

In figure 6a, the coherence has been computed on a slope interferogram, for a vertical slope. A model of building (fig 6c) has been employed to generate the source radar images through 2SIR (described in the following part). We can verify that the coherence is better in the layover region as we expected, since a signal from a vertical plane was superposed. So, a high coherence identifies a region of vertical plane, therefore a layover area. The difficulty is to choose an accurate threshold  $T_v$ .

The purpose is take into account the two slope interferograms ( $I_h$  for the horizontal slope and  $I_v$  for the vertical slope), and the two coherence image (named  $C_h$  and  $C_v$ ) to unfold the layover. We will describe a simple method in four steps to do this by travelling in the range index direction:

1. We unwrap the phase in  $I_h$  until  $C_v$  is higher than  $T_v$ . We must keep in mind that a phase plane has been subtracted.
2. The beginning of the layover is detected, we notice the position  $l_{\text{begin}}$ . Then we unwrap  $I_h$  again in the range index direction, until  $C_v$  is smaller than  $T_v$ .
3. The end of the layover is detected, we noticed this new position  $l_{\text{end}}$ . We must unwrap now  $I_v$  in the reverse order, without forget that the subtracted phase plane is different. We stop when we reach the position  $l_{\text{begin}}$ .

4. We unwrap again  $I_h$  in the normal direction without taking into account  $C_v$ . When the position  $I_{end}$  is reached again we go back to the step one.

A technical problem is that the final image of the unwrapped phase is much larger than the interferograms, and the size can not be predicted. Moreover, the distance does not still match with the index of the range direction due to the unfolding process. An other problem, is the choice of the value of  $T_v$ , but it seems that it could be predicted and modeled.

We could wonder if the algorithm would detect a layover area on a slide like in figure 6d (for example if  $T_v$  is fixed too low), but it would not! The coherence computed for a horizontal plane (figure 6b) shows that there is no signal related to a horizontal plane in this region, therefore there is no such layover. This process is indeed really accurate if there are only horizontal and vertical planes. In fact it should compute coherence for each possible slope, in order to detect each superposed slope signal before unwrapping the phase.



Fig 6a: Coherence after a vertical filtering on a building

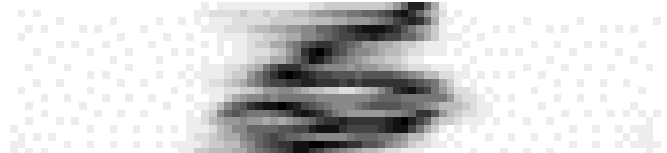
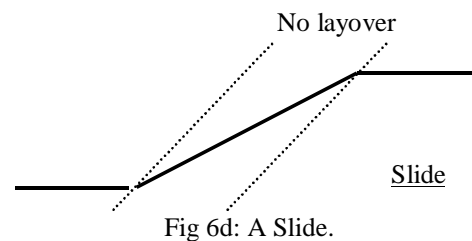
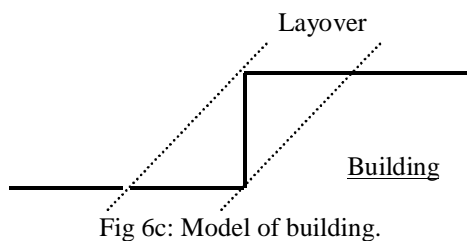


Fig 6b: Coherence after a horizontal filtering on a slide



## 5. THE SIMULATOR 2SIR

### 1 2SIR

Due to the number and the complexity of uncontrolled interactions at work in urban areas, we choose to use simulations to study the layover produced by buildings. An interferogram simulator developed at CNES, IRIT and CS, which is called 2SIR<sup>9</sup>, can achieve those. This tool has been designed in order to simulate realistic interferograms (and their pair of radar images) in such complex situations as urban areas. It uses three databases to describe the scenes, and a hybrid technique of z-buffering and ray-tracing. Those techniques allow taking into account dielectric specificities, 3D shapes, shadows, layover, surface discontinuity and double bounce.

### 2 Technical features of the simulator

The scene is described in a Terrain Object Models Data Base (TOMDB), by basic objects defined in the Object Data Base (ODB) with some properties specified in the Materials Data Base (MDB). Each element of the TOMDB consists also in two links with the two other Databases, and an object descriptor that specifies the localization and the dimensions of the object.

The images are computed in two steps (Fig. 7). First of all, targets are randomly distributed within the objects, then returned echoes are added to simulate the radar response in an intermediate angular image. The purpose of this preprocessing is to manage masked echoes (with the technique called z-buffering) and transparency, effects which can't be ignored in urban areas. The second step consists in a summation of echoes registered at the same range gate to generate the final radar image. As an intermediate angular image is computed, it allows an optical view to be processed (according to geometrical considerations).

A new version of 2SIR is used in this study. The backscattering model has benefited of a few improvements.  $\sigma_0$  is composed of a specular part and a scattering component. The parameter  $\rho_s$  specifies the specular contribution when then local angle of incidence  $\theta'$  is null. The coefficient  $\kappa$  is a roughness parameter that reduces the width of this specular part.

The scattering component is characterized by  $\rho_0$ . These three parameters are computed by fitting data extracted from the Handbook of F. T. Ulaby and M. C. Dobson<sup>10</sup>.

$$\sigma = 10 \log(\rho_s \exp(-\sin(\theta')/\kappa + \rho_0) \cos(\theta')) \quad (24)$$

Large improvements have been carried out in the model of volumic scattering, and five other parameters characterize the global backscattering model. Besides a ray-tracing module has been included in the simulator which allows now certain type of multiple bounces.

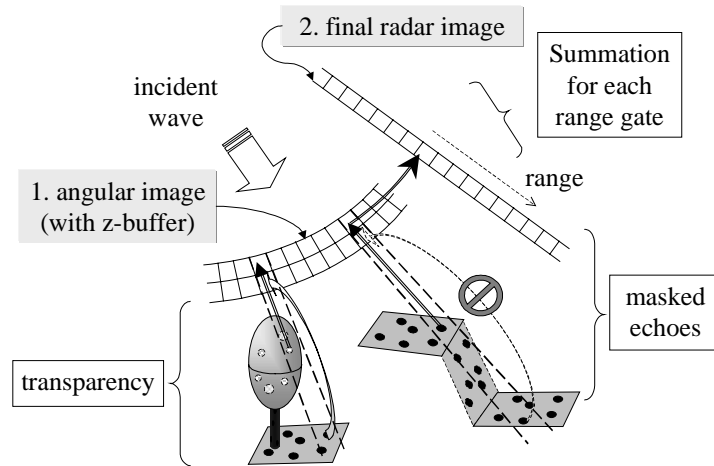


Fig. 7: The 2 steps of the image generator 2SIR.

Therefore, this application provides three types of images, such as the bare example of an urban area shown in fig. 8. The simulator 2SIR produces images of coherence and anaglyphs too. An Anaglyph grants a quick and practical perception of puzzling “3D” scenes.

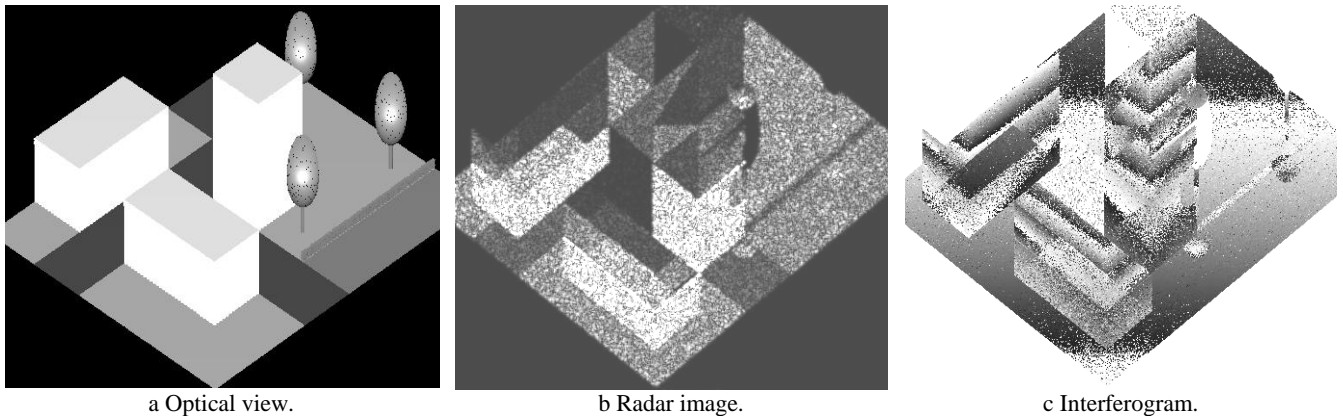


Fig.8: 3 Types of images produced by 2SIR.

### 3 Simulations

2SIR has computed simulations to test the filtering algorithm described before. We choose the X Band, with a VV polarization. The slant range and along track resolutions equal to 0.5 meters. The interferometric system is presumed bistatic. Two case have been studied:

1. We test several spectral shifts in the spatial case, with a near range of 800 km.
2. The airborne IFSAR do allow many configurations that verify (23). The results are similar to the spatial case with the same spectral shift and are not reported.

The sampling frequency  $F_s$  equal the bandwidth  $B$ . The kernel used to compute the coherence is  $[1 \ 1 \ 2 \ 1 \ 1]/6$ . It has one dimension which is extended in the along track direction.



As the Handbook of radar scattering of F.T. Ulaby<sup>10</sup> did not provide enough values for the backscattering model, an intermediate model between the road one and the rock and soil one has been used. In any case, this is the phase in which we are especially interesting.

## 6. RESULTS

### 1 Involvement of the filtering

We chose the baseline (or the altitude of ambiguity) in order to have a spectral shift of 7% of  $B$ . The height of the slide and the building is 20 meters. Whereas the 3D reconstruction is painless (fig 9a and 10a) on a slide, classical algorithms can not unwrap the phase (fig 9b) on a building (fig 10b). Although our unwrapping algorithm is unpretentious, it is obvious that no algorithms could improve significantly the results without taking into account the fact there is a layover area.

Our slope filtering algorithm obtain better results (fig 10c), in this simulation anyway. For other  $\Delta f$ , a classical algorithm can not still unwrap the phase, while our algorithm work even better (fig 10d).

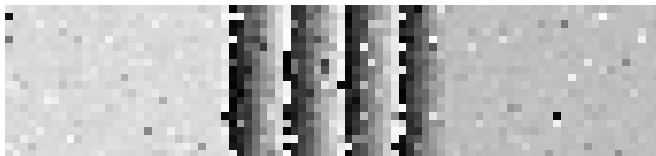


Fig 9a: Interferogram on the slide.

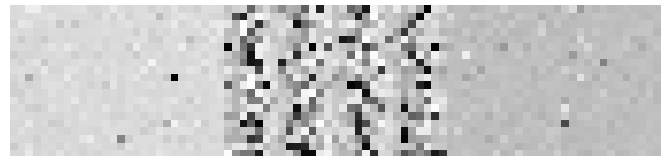


Fig 9b: Interferogram on the building.

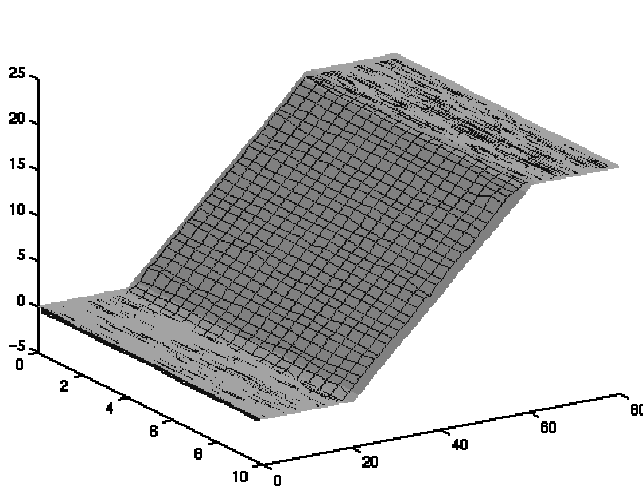


Fig 10a: The reconstructed slide.

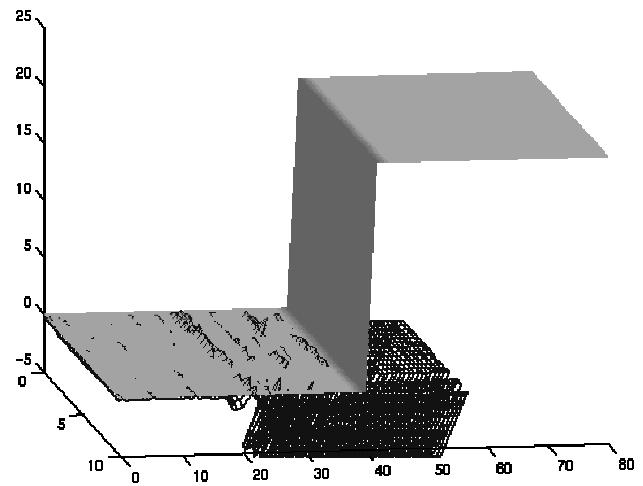


Fig 10b: The reconstructed building without filtering

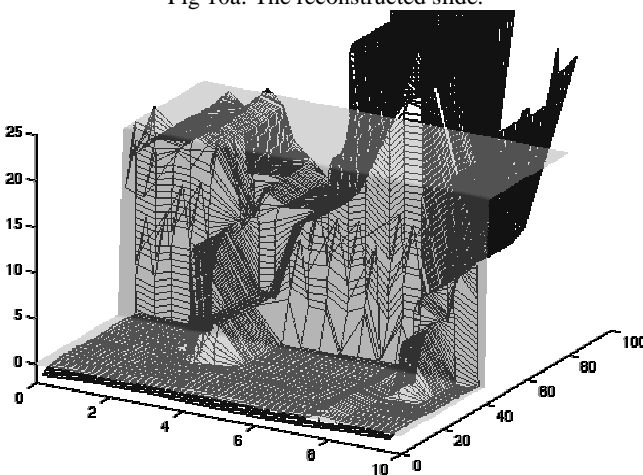


Fig 10c: The reconstructed building in case of a low spectral shift.

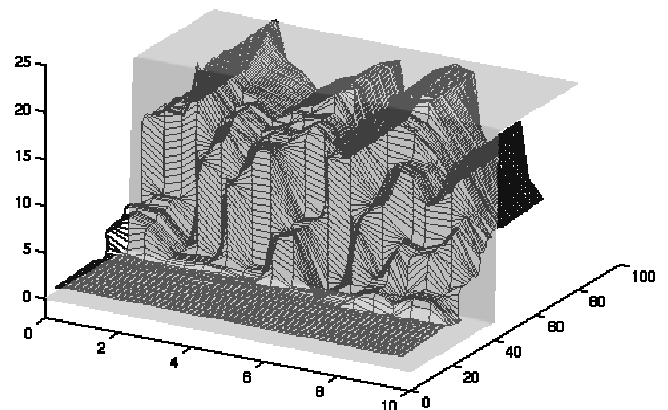


Fig 10d: The reconstructed building in case of a mean spectral shift.

## 2 The effects of the spectral shift

We compute the Root Mean Square between the assessed elevation and the true elevation for different spectral shift. The results are report in figure 11a. The required Threshold is report in figure 11b. The results seem being not as good as we expected, because the RMS we used is inaccurate. We should compute the RMS between the two surfaces rather than between two MNE. Near the front of the building, the RMS is excessive. Besides, we must keep in mind that we unwrap each line of phase individually. The results could be better, if the phase was unwrapped in each direction, but it provides us here some statistical information.

For small shifts, the resolution is highly degraded by the filtering., so the quality of the results is lesser. For important shifts, the width of the band that can match is lesser, so the coherence too. This last explanation explicates the exponential decrease of the threshold  $T_v$ , according to the spectral shift.

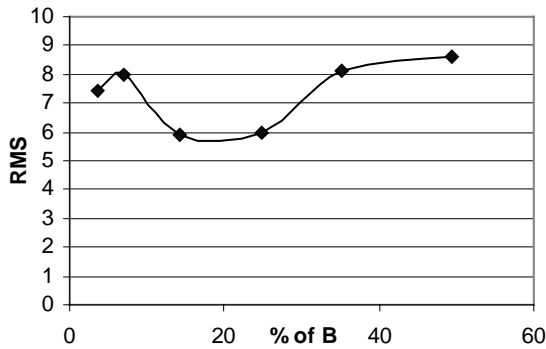


Fig. 11a: The Root Mean Square according to the spectral shift

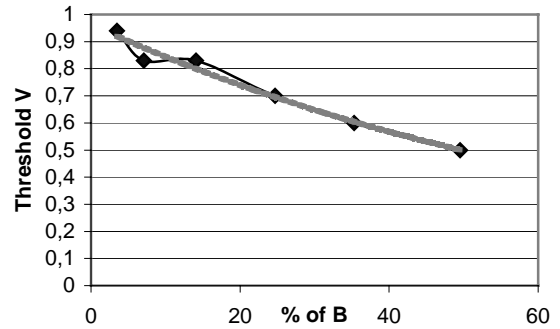


Fig. 11a: Vertical threshold according to the spectral shift

We can notice the difficulty to unwrap the building layover for important spectral shifts in figures 12a and 12b. However, The process is not well optimized, and can still be improved.

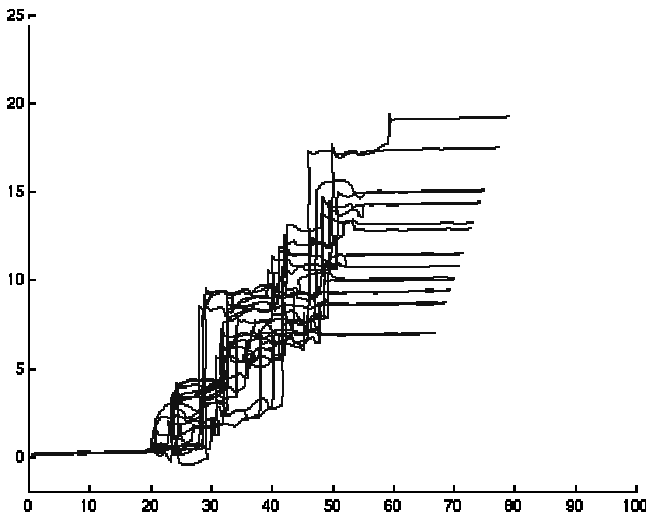


Fig 12a: Reconstructed profil of elevation for a shift of 35% of  $B$

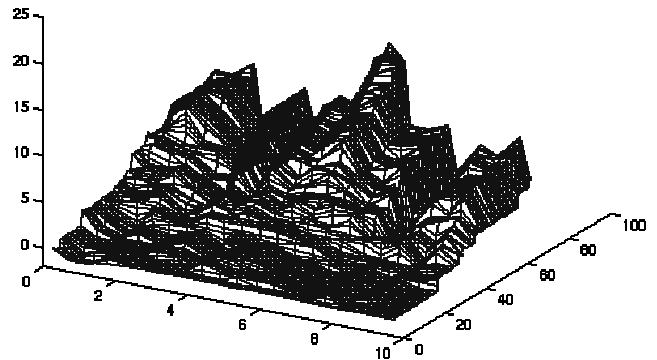


Fig 12b: reconstructed building for a shift of 50% of  $B$

## 3 Double bounce

We introduce the double bounce in certain simulation, in order to produce more realistic source radar image. It means, we have a strong echo localized at the bottom of the building. This double bounce perturbs the filtering technique. As the slope filtering degrades the resolution, the strong echo imposes its signal on large area. The computed coherence is therefore

better than we expected. So, the algorithm detects too many layover areas. The reconstructed building in figure 13 looks fine, because the surface is cut, but the RMS is 20,7 meters. Nevertheless, it may be easy to reduce the effect of the double bounce by reducing its intensity.

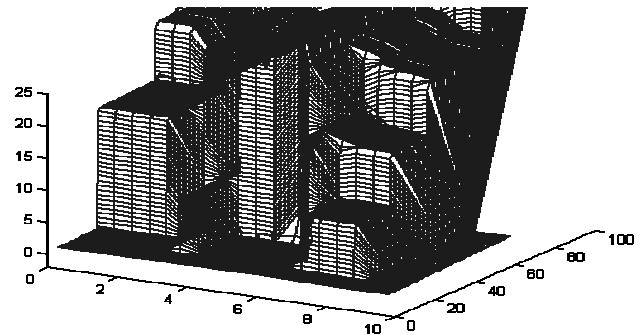


Fig. 13: The reconstructed building in the case of double bounce, for a shift of 3,5% of B.

## 7. CONCLUSIONS AND PROSPECTS

We demonstrated how to use the spectral shift to select an interferogram related to a slope. We drew a technique to separate two slope interferograms in a layover region. We described a method to unwrap the layover area produced by buildings.

The simulations showed that the slope filtering can make the most of the layover area to reconstruct the 3D shapes. This process has limitations with regard to the altitude of ambiguity. Nevertheless, it is a promising technique considering that other algorithms generally suppress layover areas since they are unable to process those regions. Moreover, the algorithm can still be improved.

We need now to test the slope filtering on real data. The double bounce may be a handicap to process suitably. Besides, it would be interesting to develop a quick analyzer, which could identify the slopes.

## 8. REFERENCES

1. P. Gamba, and B. Housmand, "Three dimensional urban characterization by IFSAR measurements", *IEEE Transactions. on Geoscience and Remote Sensing*, vol 1, pp 302-304, 1999.
2. D. L. Bickel, W. H. Hensley, and D. A. Yocky, "The effect of Scattering from Buildings on Interferometric SAR Measurements", *IEEE Transactions. on Geoscience and Remote Sensing, A Scientific Vision for Sustainable Development*, vol. 4, pp 1545-1547, 1997.
3. C. Prati, and F. Rocca, "Improving slant range resolution of stationary objects with multiple SAR surveys.", *IEEE Transactions on Aerospace Electronic System*, vol. 29, pp. 135-144, Jan. 1993.
4. F. Gatelli, A. Monti Guarnieri, F. Parizzi, P. Pasquali, and C. Prati, "The wavenumber shift in SAR Interferometry", *IEEE Transactions. on Geoscience and Remote Sensing*, vol. 32, no. 4, pp. 855-865, July 1994.
5. F. Adragna, "Interférométrie radar : Principes, applications et Limitations", *Bulletin de la Société Française de Photogrammétrie et Télédétection*, n° 148, pp. 15-19, 1997-4.
6. D. Massonnet, "Producing ground deformation maps automatically; the DIAPASON concept", *IEEE Transactions. on Geoscience and Remote Sensing, A Scientific Vision for Sustainable Development*, vol. 3, pp 1338-1340, 1997.
7. D. Massonnet, "Interférométrie par radar", CT/PF/TI/AS n°249 (internal memo), 16.09.1985
8. A.J. Wilkinson, "Synthetic aperture radar interferometry: a statistical model for layover areas.", *IEEE Transactions. on Geoscience and Remote Sensing*, vol. 5, pp 2392-2394, 1999.
9. D. Petit, and F. Adragna, "A new interferogram simulator: 2SIR. Study of coherence losses for tortured reliefs." *CEOS SAR Workshop*, pp 591-596, Toulouse, France, October, 1999.
10. F.T. Ulaby, M. C. Dobson, *Hanbook of radar scattering for terrain*, Artech House editor.